A Cascade MPC-Feedback Linearizing Strategy for the Multivariable Control of Animal Cell Cultures

Mihaela Sbarciog * **Daniel Coutinho** ** **Alain Vande Wouwer** *

* *Automatic Control Laboratory, University of Mons, Boulevard Dolez 31, B-7000 Mons, Belgium (e-mail: {MihaelaIuliana.Sbarciog, Alain.VandeWouwer}@umons.ac.be).*
** *Department of Automation and Systems, Federal University of Santa Catarina, 476 Florianopolis, 88040-900, Brazil (e-mail: Coutinho@das.ufsc.br)*

Abstract: In this study, a multivariable control structure is developed to simultaneously control the concentrations of cells and of one of the nutrients in an animal cell cultivation system operated in perfusion. A cascade control structure is considered consisting of (i) an inner loop with a partially linearizing feedback controller, tuned so as to ensure robustness with respect to parameter uncertainties and non-canceled nonlinearities; and (ii) an outer loop involving two linear predictive controllers. The resulting control strategy shows robustness and performance properties similar to more computationally demanding strategies (such as a multivariable nonlinear MPC strategy), while requiring less measurements and involving an easier implementation.

Keywords: biotechnology, control system design, multivariable feedback control, cascade control, feedback linearization, predictive control

1. INTRODUCTION

High-value bioproducts such as vaccines, recombinant proteins and antibodies, are used in the treatment of several diseases such as diabetes, arthritis, multiple sclerosis, cancer, anaemia and HIV (Nolan and Lee, 2011). The production of these bioproducts is delicate and in some cases the only useful in vitro process available is the cultivation of cells that are programmed to synthesize them. These cells can grow in suspension in stirred tank reactors, which appear to be the most common practice in industry for large production (Jain and Kumar, 2008). The efforts for increasing the culture productivity in these systems focus on elaborating specific culture media, and in optimal feeding policies. The most popular operating modes in cell cultures are batch, fed-batch and perfusion modes (Jain and Kumar, 2008; Komolpis et al., 2010). Batch and fed-batch modes do not offer many options for control, except for the feed rate in the latter, and the cells growth can be inhibited by the accumulation of toxic metabolites, which cannot be removed. In perfusion mode, fresh medium is fed to replenish the consumed nutrients, while an equal volume of spent medium is continuously withdrawn, allowing for the removal of inhibitory components. Cells are retained or recycled back to the reactor by some type of retention device (for instance an acoustic filter). Higher cell concentrations and higher productivity can be achieved in perfusion cultures than in conventional batch cultures (Komolpis et al., 2010). Hence perfusion processes provide consistent culture conditions, high productivity and low product residence times. However, a successful perfusion culture requires tight control of the perfusion rate. Too low perfusion rates may result in nutrient limitation, accumulation of inhibitory metabolites and retardation in cell growth rate. Too high perfusion rates may result in wash out of the cells in systems with partial cell retention. The removal of a small amount of cells from the reactor through the cell-containing flow (the bleed) is necessary for maintaining the viability of the culture, as well as for reaching steady state operation (Banik and Heath, 1995; Ozturk et al., 1997; Dalm et al., 2004).

In spite of providing increased productivity of the culture, perfusion operation with partial cell retention is hardly used at industrial scale because of the complexity raised by the multivariable nature of the process. Although several studies exist regarding the necessity and the influence of the bleed stream on the cells growth, it is not clear yet how to set this process input and how to use it for control and optimization purposes. Moreover, most of published control studies focus only on manipulating the perfusion rate (Ozturk et al., 1997; Dowd et al., 2001a).

Recently, the potential of using the bleed flow in multivariable control structures has been investigated in several simulation studies in view of a prospective practical implementation: Deschênes et al. (2006a,b) have developed an adaptive backstepping strategy for a simple model to simultaneously control the cell and metabolite concentrations, while Sbarciog et al. (2012) have designed a multivariable nonlinear predictive control strategy based on a more realistic model, for accelerating the growth of cells and controlling the substrate concentration in the effluent.

In this paper, our objective is to simplify and robustify the above-mentioned control strategy. To this end, a cascade control structure is proposed, where the dilution and the bleed rates are manipulated to control the cell and substrate concentrations. This structure combines a partial feedback linearizing controller in the inner loop, whose resulting free linear dynamics is designed to ensure robustness with respect to parametric uncertainties and non-canceled nonlinearities, with linear pre-

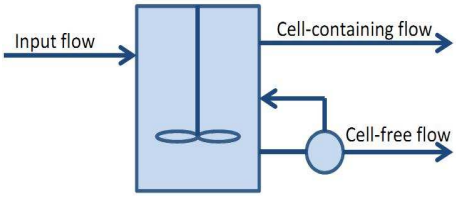

Fig. 1. Schematic representation of the perfusion culture

dictive controllers in the outer loop. Robust and predictive controllers (Dowd et al., 2001a,b; Aehle et al., 2012) are the most encountered techniques for cell culture control. Robustness is needed to cope with the culture variability and sensitivity to environmental conditions or to alleviate the negative effect of the incomplete understanding of the intricate relationship between process parameters and outputs. On the other hand, predictive control is one of the few advanced techniques which is widely accepted in industry and deals with the optimization of cell growth processes in a straightforward manner. However, direct application of predictive control to the nonlinear cell growth process is still raising controversies among practitioners, as aside the process dynamics, the involved nonlinear optimization adds complexity to the control loop. Therefore, we propose in this work an easy-to-implement control structure without trading performance for simplicity. Assuming the measurement of biomass and substrate concentrations (which are nowadays technically available in cell cultures), the partial linearizing feedback controller ensures decoupling between the inputs and the two controlled variables, with linear or quasi-linear dynamics. These are subsequently used by two linear MPC (Model Predictive Control) controllers to compute the inputs for the inner loop controller. Provided that a non-constrained optimization is solved, analytic expressions for the inner-loop controller inputs can be derived.

The paper is organized as follows: Section 2 presents the animal cell growth process, while Section 3 introduces the design of the control structure. The simulation results are shown and discussed in Section 4. The conclusions and future research perspectives are highlighted in the last Section.

2. PROCESS MODEL

The animal cell culture considered in this study is described by a model, which expresses that the cells growth is activated by the presence of glucose and glutamine and their death is governed by lactate, ammonia and glutamine concentrations. A schematic representation of the perfusion culture is given in Figure 1. Medium containing glucose and glutamine is continuously supplied to the reactor. Components leave the reactor at the same rate. The amount of cells in the effluent is determined by the filtration device.

The mathematical model of the system illustrated in Figure 1 is given by:

$$\dot{\xi}_1 = -bl \cdot D\xi_1 + r_1(\xi) - r_2(\xi) \quad (1)$$

$$\dot{\xi}_2 = D(\xi_{in_2} - \xi_2) - ar_1(\xi) - r_3(\xi) \quad (2)$$

$$\dot{\xi}_3 = D(\xi_{in_3} - \xi_3) - br_1(\xi) \quad (3)$$

$$\dot{\xi}_4 = -D\xi_4 + cr_1(\xi) + dr_3(\xi) \quad (4)$$

$$\dot{\xi}_5 = -D\xi_5 + er_1(\xi) \quad (5)$$

where

- $\xi_1, \xi_2, \xi_3, \xi_4, \xi_5$ respectively represent the concentrations of viable cells, glucose, glutamine, lactate and ammonia. ξ_{in_2} and ξ_{in_3} are the concentrations of glucose and glutamine in the influent;
- $D = F/V$ is the dilution/perfusion rate and $bl \in [0, 1]$ is the bleed ratio;
- $r_i(\xi)$, $i = 1, 2, 3$ are reaction rates, given by:

$$r_1(\xi) = \mu_{max} \cdot \frac{\xi_2}{K_{Glc} + \xi_2} \cdot \frac{\xi_3}{K_{Gln} + \xi_3} \cdot \xi_1 = \mu_1(\xi) \cdot \xi_1 \quad (6)$$

$$r_2(\xi) = \frac{k_{d_{max}}}{(\mu_{max} - k_{d_{Lac}}\xi_4)(\mu_{max} - k_{d_{Amm}}\xi_5)} \cdot \frac{k_{d_{Gln}}}{k_{d_{Gln}} + \xi_3} \cdot \xi_1 = \mu_2(\xi) \cdot \xi_1 \quad (7)$$

$$r_3(\xi) = m_{Glc} \cdot \frac{\xi_2}{k_{m_{Glc}} + \xi_2} \cdot \xi_1 = \mu_3(\xi) \cdot \xi_1 \quad (8)$$

- $a, b, c, d, e > 0$ are the stoichiometric coefficients, defined as: $a = \frac{1}{Y_{X_v/Glc}}$, $b = \frac{1}{Y_{X_v/Gln}}$, $c = \frac{Y_{Lac/Glc}}{Y_{X_v/Glc}}$, $d = Y_{Lac/Glc}$, $e = \frac{Y_{Amm/Gln}}{Y_{X_v/Gln}}$.

This model has been developed from batch and fed-batch hybridoma culture results (de Tremblay et al., 1992), with the model parameters given in Table 1.

Table 1. Numerical values of the animal cell culture (as in de Tremblay et al. (1992))

$Y_{X_v/Glc}$	$1.09 \cdot 10^2$	10^6 cells/mmol
$Y_{X_v/Gln}$	$3.8 \cdot 10^2$	10^6 cells/mmol
$Y_{Lac/Glc}$	1.8	mmol/mmol
$Y_{Amm/Gln}$	0.85	mmol/mmol
μ_{max}	1.09	d^{-1}
$k_{d_{max}}$	0.69	d^{-1}
V	0.8	L
K_{Glc}	1	mmol/L
K_{Gln}	0.3	mmol/L
$k_{d_{Lac}}$	0.01	d^{-1}(mmol/L)$^{-1}$
$k_{d_{Amm}}$	0.06	d^{-1}(mmol/L)$^{-1}$
$k_{d_{Gln}}$	0.02	mmol/L
m_{Glc}	$1.68 \cdot 10^{-4}$	mmol(10^6 cells)$^{-1}d^{-1}$
$k_{m_{Glc}}$	19	mmol

3. CONTROL STRUCTURE DESIGN

The main objective is to achieve and maintain a high cell density in the reactor. Naively, supplying high amounts of substrates determines a better and faster growth of the cells. In practice however (Jain and Kumar, 2008), this leads to an inefficient use of the medium and it is detrimental to the cells, as large amounts of expensive nutrients are lost via the effluent and toxic byproducts causing cell death are produced. Therefore, many control implementations consider the regulation of the main nutrient glucose at a reasonable low level to minimize the formation of toxic metabolites (Dowd et al., 2001b; Ozturk et al., 1997; Yang et al., 2000). In this paper we design the control structure to achieve a similar goal, i.e., the regulation of cell and glucose concentrations at specified setpoints.

Thus, the control goal is to manipulate the dilution rate D and the bleed ratio bl (or equivalently the bleed rate defined as $D_b = bl \cdot D$) such that the biomass concentration ξ_1 and the glucose concentration ξ_2 follow their setpoints defined by ξ_1^{ref},

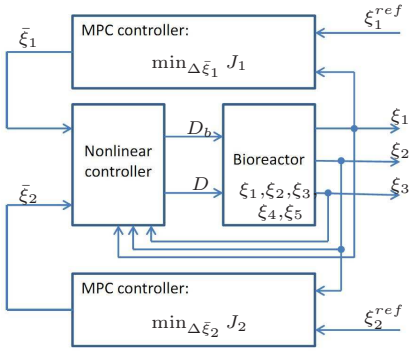

Fig. 2. Control structure

ξ_2^{ref}. This goal is achieved by a cascade control structure as illustrated in Figure 2: (i) a partial feedback linearizing controller is designed such that the inner loop has approximately a decoupled linear dynamics; and (ii) two linear MPC controllers are used in the outer loops to compute the inputs of the inner loop controller $\bar{\xi}_1$, $\bar{\xi}_2$.

3.1 Inner loop controller

The inner loop controller is a partial feedback linearizing controller, which considers the measurement of ξ_1, ξ_2 and ξ_3. The control law is given by:

$$D_b = bl \cdot D = \frac{1}{\xi_1}\left(r_1(\xi) - \lambda_1(\bar{\xi}_1 - \xi_1)\right) \tag{9}$$

$$D = \frac{1}{(\xi_{in_2} - \xi_2)}\left(a \cdot r_1(\xi) + r_3(\xi) + \lambda_2(\bar{\xi}_2 - \xi_2)\right) \tag{10}$$

where λ_1, λ_2 are the controller parameters (to be tuned) and $\bar{\xi}_1$, $\bar{\xi}_2$ are the controller inputs.

For designing the controller parameters λ_1 and λ_2, we consider that the model (1)-(5) is not perfectly known. In this paper, it is assumed that μ_{max} may vary $\pm$ 20 % with respect to its nominal value, that is:

$$\mu_{max} = \mu_{max}(\delta) = \bar{\mu}_{max}(1 + 0.2\delta)\ ,\ \delta \in [-1, 1]\ , \tag{11}$$

where $\bar{\mu}_{max}$ stands for the nominal value of μ_{max} and δ is an uncertain parameter lying in the interval $[-1, 1]$. Notice that we cannot straightforwardly implement the control law given in (9)-(10), because μ_{max} is uncertain. To overcome this problem, we estimate the value of $r_1(\xi) = r_1(\xi, \delta)$ based on the nominal value of μ_{max} leading to

$$D_b = \frac{1}{\xi_1}\left(\hat{r}_1(\xi) - \lambda_1(\bar{\xi}_1 - \xi_1)\right) \tag{12}$$

$$D = \frac{1}{(\xi_{in_2} - \xi_2)}\left(a \cdot \hat{r}_1(\xi) + r_3(\xi) + \lambda_2(\bar{\xi}_2 - \xi_2)\right) \tag{13}$$

where

$$\hat{r}_1(\xi) = \bar{\mu}_{max} \cdot \frac{\xi_2}{K_{Glc} + \xi_2} \cdot \frac{\xi_3}{K_{Gln} + \xi_3} \cdot \xi_1 \tag{14}$$

Using (12) and (13) in the model (1)-(5) and defining

$$\chi_1 = \bar{\xi}_1 - \xi_1\ ,\ \chi_2 = \bar{\xi}_2 - \xi_2\ ,$$

the following dynamics for the controlled outputs is obtained:

$$\dot{\chi}_1 = -\lambda_1\chi_1 - \left(r_1(\xi, \delta) - \hat{r}_1(\xi)\right) + r_2(\xi) \tag{15}$$

$$\dot{\chi}_2 = -\lambda_2\chi_2 + a\left(r_1(\xi, \delta) - \hat{r}_1(\xi)\right) \tag{16}$$

Notice that the above dynamics is not linear since the term $r_1(\xi, \delta) - \hat{r}_1(\xi)$ is not canceled due to parameter uncertainty and $r_2(\xi)$ is not considered in the feedback linearizing based controller to avoid additional measurements.

Thus, we design λ_1 and λ_2 to minimize the effects of the non-canceled nonlinearities in (15)-(16) on the state vector $\chi := [\chi_1\ \chi_2]^T$ in the $\mathcal{H}_\infty$ sense. To this end, we embed (15)-(16) into the following *quasi*-LPV representation (Leith and Leithead, 2000):

$$\mathcal{G}_{wz} : \left\{\dot{\chi} = \begin{bmatrix} \lambda_1 & 0 \\ 0 & \lambda_2 \end{bmatrix}\chi + \begin{bmatrix} 0.2\delta & 1 \\ 0.2a\delta & 0 \end{bmatrix} w\ ,\ z = \chi \right. \tag{17}$$

where the disturbance input w models the non-canceled dynamics, that is:

$$w := \begin{bmatrix} \dfrac{\bar{\mu}_{max}\xi_1\xi_2\xi_3}{(K_{Glc} + \xi_2)(K_{Gln} + \xi_3)} \\ r_2(\xi) \end{bmatrix}$$

Then, the parameters λ_1 and λ_2 are designed to minimize an upper-bound on $\|\mathcal{G}_{wz}\|_\infty$ for all $\delta \in [-1, 1]$ using similar steps as in the approach proposed in (Dewasme et al., 2011).

Notice that the overall feedback system aims at operating in set point regions such that the death rate $r_2(\xi)$ is close to zero. In addition, if $\|\mathcal{G}_{wz}\|_\infty$ is relatively small, we may also assume that $\Delta r_1 := r_1(\xi, \delta) - \hat{r}_1(\xi) \simeq 0$. Hence, to determine the inner-loop controller inputs $\bar{\xi}_1$ and $\bar{\xi}_2$ in the MPC setting, as proposed in the next section, the following simplified dynamics is considered:

$$\dot{\bar{\xi}}_1 = \lambda_1\left(\bar{\xi}_1 - \xi_1\right) \tag{18}$$

$$\dot{\bar{\xi}}_2 = \lambda_2\left(\bar{\xi}_2 - \xi_2\right) \tag{19}$$

3.2 Outer-loop controllers

Two simple controllers are designed to compute the inputs of the inner-loop controller using the key components of the MPC strategy (Camacho and Bordons, 1999): a model used for prediction, an online optimization and the feedback compensation. The models used for prediction by each MPC controller are built on the consideration that the measured system output is the combined contribution of the system dynamics and process disturbance. Hence the models assume the form

$$\xi_i^m(t) = \frac{B_i\left(q^{-1}\right)}{A_i\left(q^{-1}\right)}\bar{\xi}_i(t) + \frac{C_i\left(q^{-1}\right)}{D_i\left(q^{-1}\right)}e(t), \quad i = 1, 2 \tag{20}$$

where ξ_1^m, ξ_2^m are the models outputs; $A_i\left(q^{-1}\right)$, $B_i\left(q^{-1}\right)$ are polynomials in the shift operator q found by discretizing respectively the dynamics (18), (19) with a sampling period T_s; $C_i\left(q^{-1}\right)$, $D_i\left(q^{-1}\right)$ are polynomials in the shift operator q, with $\dfrac{C_i\left(q^{-1}\right)}{D_i\left(q^{-1}\right)}$ representing the disturbance model; $e(t)$ is uncorrelated noise with zero mean value. As no particular information on the process disturbance is known, the default structure for the disturbance models is considered, i.e.:

$$\frac{C_i\left(q^{-1}\right)}{D_i\left(q^{-1}\right)} = \frac{1}{1 - q^{-1}}\ .$$

The standard GPC (Generalized Predictive Control) algorithm is employed: it is assumed that the control effort is of the form

$$\bar{\xi}_i(t) = \bar{\xi}_i(t-1) + \Delta\bar{\xi}_i(t), \qquad i = 1, 2 \tag{21}$$

Then the predicted system outputs over the prediction horizon N_p by considering N_u control moves are calculated as the sum of the free and forced responses

$$\hat{\xi}_i^m = \tilde{\xi}_i^m + G_i\Delta\bar{\xi}_i \tag{22}$$

where $\hat{\xi}_i^m \in \mathbb{R}^{N_p \times 1}$; $\tilde{\xi}_i^m \in \mathbb{R}^{N_p \times 1}$ is computed on the horizon N_p by setting $\bar{\xi}_i$ to the last derived control effort $\bar{\xi}_i(t-1)$ in (20); $\Delta\bar{\xi}_i \in \mathbb{R}^{N_u \times 1}$ are the control increments to be determined; $G_i \in \mathbb{R}^{N_p \times N_u}$ is the matrix of unit step response coefficients, having the structure

$$G_i = \begin{pmatrix} g_i^1 & 0 & \dots & 0 \\ g_i^2 & g_i^1 & \dots & 0 \\ \vdots & \vdots & \vdots & \vdots \\ g_i^{N_p} & g_i^{N_p-1} & \dots & g_i^{N_p-N_u+1} \end{pmatrix}$$

Each of the control increments $\Delta\bar{\xi}_i$ is calculated by minimizing the cost index

$$J_i = \left(\xi_i^{ref} - \hat{\xi}_i^m\right)^T \cdot \left(\xi_i^{ref} - \hat{\xi}_i^m\right) + \alpha_i \left(\Delta\bar{\xi}_i\right)^T \cdot \left(\Delta\bar{\xi}_i\right) \quad (23)$$

Using (22) in (23) an analytical expression of the control increments may be obtained:

$$\Delta\bar{\xi}_i = \left(G_i^T G_i + \alpha_i I\right)^{-1} G_i^T \left(\xi_i^{ref} - \tilde{\xi}_i^m\right) \quad (24)$$

4. SIMULATIONS AND DISCUSSION

In order to implement the proposed control structure, one needs to off-line:

- compute the gains λ_1, λ_2 of the inner-loop controller;
- obtain the discrete time models of the linear dynamics and calculate the unit step responses.

Then, at each sampling instant:

- biomass, glucose and glutamine concentrations are measured;
- a prediction of the inner loop behavior is calculated over the prediction horizon N_p based on the models (20);
- the cost functions (23) are minimized;
- the new control inputs of the inner-loop controller are found and the new values for the dilution and bleed rates are calculated;
- the newly found process inputs may be clipped to comply with the physical constraints on the dilution and bleed rates: $0 \leq D \leq 3.75\text{d}^{-1}$, $0 \leq D_b \leq D$.

Simulation results of the proposed control loop are presented in Figures 3, 4 and 5. The parameters of the inner-loop controller are set to $\lambda_1 = 11.8319$, $\lambda_2 = 6.9534$, while for the MPC controllers the prediction and control horizons N_p, N_u are respectively set to 15 and 1. A sampling period of 0.05d is used. Figure 3 shows the control results for the nominal values of the process parameters, while Figures 4 and 5 show the closed-loop response for respectively an increase and a decrease of 20% on the maximum growth rate μ_{max}. The simulation results presented here include: the controlled outputs ξ_1, ξ_2 and their respective setpoints; the inputs of the inner-loop controller computed by the two MPC controllers represented with continuous line and the inputs which are admissible (to comply with the physical constraints on the flow rates) represented with dashed line; the process inputs calculated by the inner-loop controller: the dilution and the bleed rates.

A good behavior is achieved in closed loop, even in the presence of parameter uncertainty, as both outputs follow closely the imposed setpoint changes and reach the steady state almost simultaneously. The control efforts change smoothly, due to the penalty on the control moves in the optimization criteria (23) (introduced to compensate for solving unconstrained optimization problems). Although penalizing the slew rate is common in MPC, here it was introduced to keep the complexity of the implementation low, as the relationships between the dilution and bleed rates and the inner-loop controller inputs are nonlinear. Thus, in order to avoid solving optimization problems with nonlinear constraints, one needs to properly select the penalty weights α_1, α_2. For the simulation results presented in Figure 3, $\alpha_1 = 150$, $\alpha_2 = 100$ for $t \leq 20$d and $\alpha_1 = 220$, $\alpha_2 = 200$ for $t > 20$d. Similarly, for the results shown in Figures 4 and 5, $\alpha_1 = 150$, $\alpha_2 = 100$ for $t \leq 10$d and $\alpha_1 = 200$, $\alpha_2 = 120$ for $t > 10$d.

The tuning of the cascade control structure is equivalent to tuning the MPC controllers, where appropriate values for the control and prediction horizons and for the penalty factors must be selected. While general guidelines exist for choosing the horizons N_u, N_p, some insight of the process dynamics is needed to select appropriately the penalties α_1, α_2. These weighting coefficients provide a means to cope with the constraints on the physical inputs, but at the same time they increase the robustness with respect to the non-cancelled nonlinearities. The selection of setpoints corresponding to high cells concentration and low glucose concentration (eg. Figure 3) leads inherently to the increase of the death rate, which may become comparable to the growth rate (such as illustrated in Figure 6). In these cases, the assumption that the death rate is close to zero does not hold and the model used by the MPC controllers is not accurate. However, as shown in Figures 3-5, increasing the weighting coefficients leads to the successful implementation of the proposed control structure.

In order to assess the performance of the proposed cascade control structure, the closed-loop response is compared to the one obtained using a multivariable nonlinear predictive controller as proposed, for instance, in (Sbarciog et al., 2012). This nonlinear predictive control implementation uses the full system model to compute the output predictions, assuming thus the availability of the full system state. The optimal dilution and bleed rates are determined by minimizing the cost index (23), for $i = 1, 2$, in an iterative manner, thus implying a higher computational effort. Figures 3- 5 show that the proposed control structure produces results at least as good as the nonlinear predictive controller; however it requires less measurements and the computational effort is minimum if compared to the nonlinear MPC, advantages which make the cascade control structure a potential candidate for real-life applications.

5. CONCLUSION

In this paper the design and implementation of a cascade control structure for an animal cell culture has been presented. The control loop, comprising a partially linearizing feedback controller and two SISO linear predictive controllers, is an effective and easily implementable solution, which allows the simultaneous control of the biomass and substrate concentrations while ensuring robustness with respect to parametric uncertainties and non-canceled nonlinearities. Further developments include the real-life application of the proposed control structure on an animal cell culture.

ACKNOWLEDGEMENTS

The authors gratefully acknowledge the support of the FEDER program 2007-2013, in the framework of Hainaut-Biomed, and

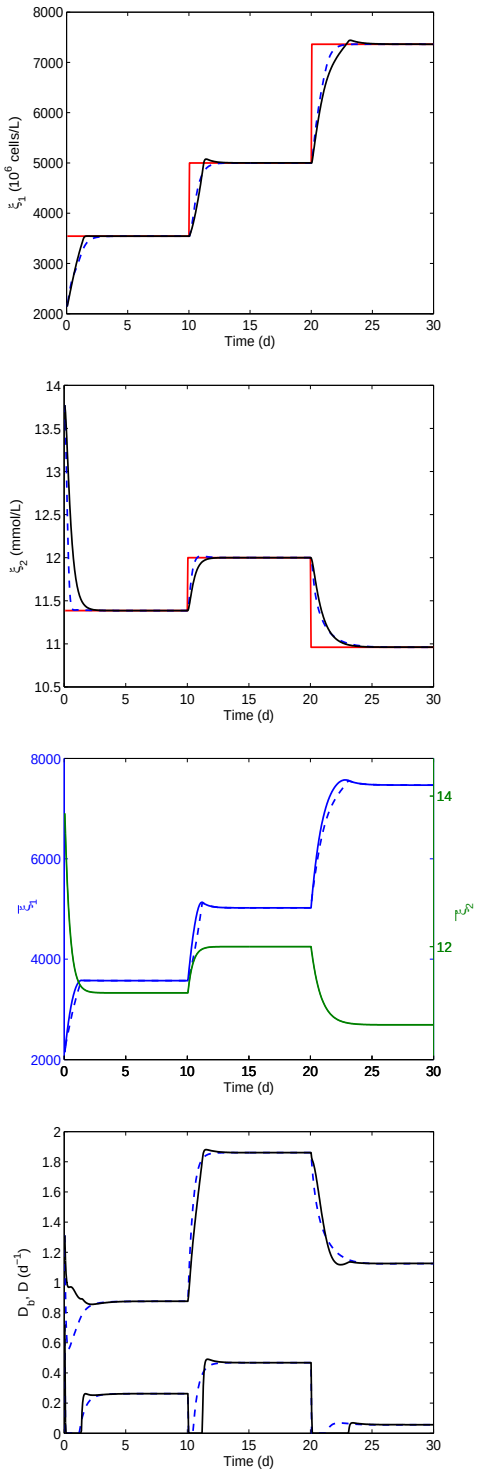

Fig. 3. Closed loop response: the proposed strategy (continuous line), nonlinear MPC (dashed line)

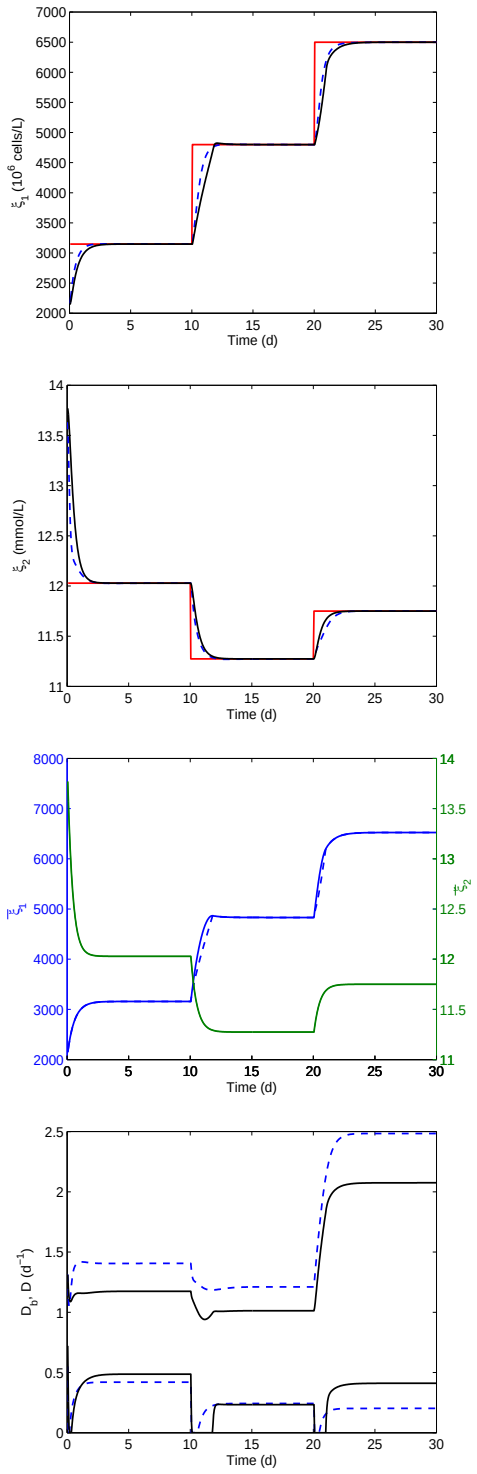

Fig. 4. Closed loop response for a 20% increase in the maximum specific growth μ_{max}: the proposed strategy (continuous line), nonlinear MPC (dashed line)

the research project OCPAM. This paper presents research results of the Belgian Network DYSCO (Dynamical Systems, Control, and Optimization), funded by the Interuniversity Attraction Poles Programme, initiated by the Belgian State, Science Policy Office. The authors also gratefully acknowledge the support of FNRS and CNPq in the framework of a bilateral research project led by Paul Van Dooren (UCL, Belgium) and Carlos E. de Souza (LNCC, Brazil). The scientific responsibility rests with the author(s).

REFERENCES

Aehle, M., Bork, K., Schaepe, S., Kuprijanov, A., Horstkorte, R., Simutis, R., and Lübbert, A. (2012). Increasing batch-to-batch reproducibility of cho-cell cultures using a model predictive control approach. *Cytotechnology*, 64, 623–634.

Banik, G. and Heath, C. (1995). Partial and total cell retention in a filtration base homogeneous perfusion reactor. *Biotechnology Progress*, 11, 584–588.

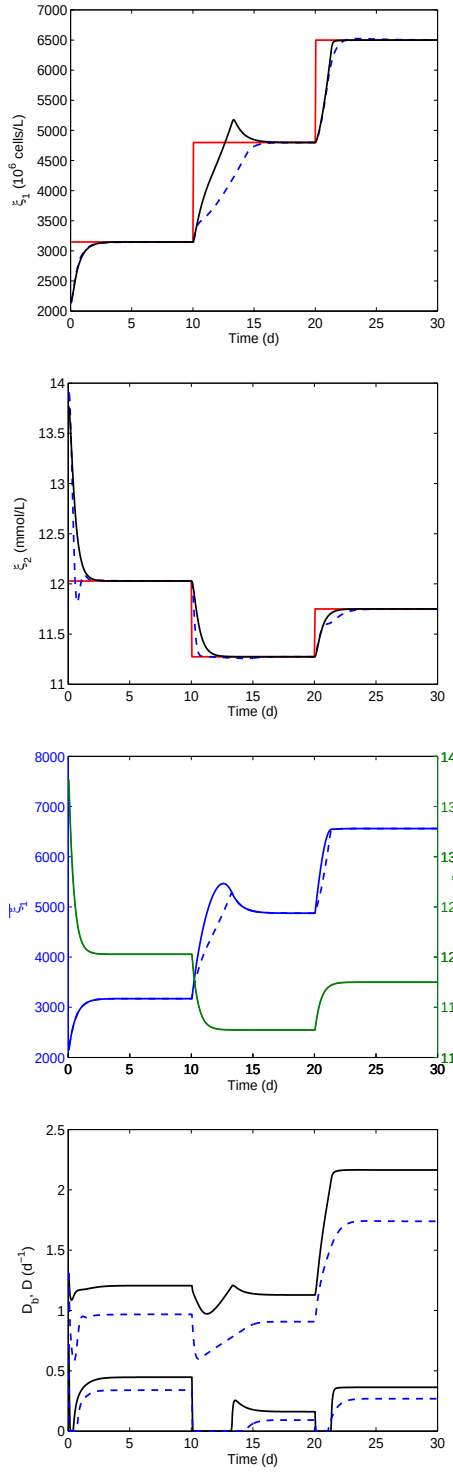

Fig. 5. Closed loop response for a 20% decrease in the maximum specific growth μ_{max}: the proposed strategy (continuous line), nonlinear MPC (dashed line)

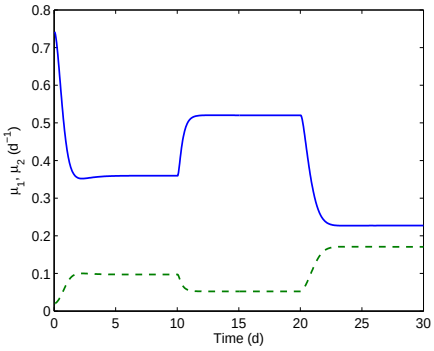

Fig. 6. Growth (continuous line) and death (dashed line) rates corresponding to the simulation results shown in Figure 3

using dynamic programming: single and multi feed cases. *Bioprocess Engineering*, 7, 229–234.

Deschênes, J.S., Desbiens, A., Perrier, M., and Kamen, A. (2006a). Multivariable nonlinear control of biomass and metabolite concentrations in a high-cell-density perfusion bioreactor. *Ind. Eng. Chem. Res.*, 45, 8985–8997.

Deschênes, J.S., Desbiens, A., Perrier, M., and Kamen, A. (2006b). Use of cell bleed in a high cell density perfusion culture and multivariable control of biomass and metabolite concentrations. *Asia-Pac. J. Chem. Eng*, 1, 82–91.

Dewasme, L., Coutinho, D., and Vande Wouwer, A. (2011). Adaptive and robust linearizing control strategies for fed-batch cultures of microorganisms exhibiting overflow metabolism. In J.A. Cetto, J.L. Ferrier, and J. Filipe (eds.), *Informatics in Control, Automation and Robotics*, volume LNEE 89, 283–305. Spinger.

Dowd, J., Kwok, K., and Piret, J. (2001a). Glucose-based optimization of CHO-cell perfusion cultures. *Biotechnology & Bioengineering*, 75, 252–256.

Dowd, J., Kwok, K., and Piret, J. (2001b). Predictive modeling and loose-loop control for perfusion bioreactors. *Biochemical Engineering Journal*, 9, 1–9.

Jain, E. and Kumar, A. (2008). Upstream processes in antibody production: Evaluation of critical parameters. *Biotechnology Advances*, 26, 46–72.

Komolpis, K., Udomchokmongkol, C., Phutong, S., and T.Palaga (2010). Comparative production of a monoclonal antibody specific for enrofloxacin in a stirred-tank bioreactor. *Journal of Industrial and Engineering Chemistry*, 16, 567–571.

Leith, D.J. and Leithead, W.E. (2000). Survey of gain-scheduling analysis and design. *International Journal of Control*, 73, 1001–1025.

Nolan, R. and Lee, K. (2011). Dynamic model of cho cell metabolism. *Metabolic Engineering*, 3, 108–124.

Ozturk, S., Thrift, J., Blackie, J., and Naveh, D. (1997). Real-time monitoring and control of glucose and lactate concentrations in a mammalian cell perfusion reactor. *Biotechnology & Bioengineering*, 53, 372–378.

Sbarciog, M., Saraiva, I., and Vande Wouwer, A. (2012). Accelerating animal cell growth in perfusion mode by multivariable control: Simulation studies. *Bioprocess and Biosystems Engineering*, in press.

Yang, J., Angelillo, Y., Chaudhry, M., Goldenberg, C., and Goldenberg, D. (2000). Achievement of high cell density and high antibody productivity by a controlled-fed perfusion bioreactor process. *Biotechnology & Bioengineering*, 69, 74–82.